Shear Behavior of Reinforced Concrete Shear Walls under Tensile Axial Force with Eccentricity

著者	MIZOGUCHI Mitsuo, ARAI Yasuyuki, KUCHIJI Hideki
journal or publication title	Transactions of the Japan Concrete Institute
volume	22
page range	369-376
year	2000-02
URL	http://hdl.handle.net/10258/1283

SHEAR BEHAVIOR OF REINFORCED CONCRETE SHEAR WALLS UNDER TENSILE AXIAL FORCE WITH ECCENTRICITY

Mitsuo MIZOGUCHI*1, Yasuyuki ARAI*1 and Hideki KUCHIJI*2

ABSTRACT

A lateral loading test of six reinforced concrete shear walls subjected to an eccentric tensile axial force was carried out to examine their shear behavior. Next, facts were confirmed on the shear strength of the walls subjected to an eccentric tensile axial force. The test results can be evaluated by the shear strength equation [2] considering axial tensile stress. The calculated values given by the (AIJ "Design Guidelines for Earthquake Resistant Reinforced Concrete Buildings Based on Inelastic Displacement Concept") equation [3] are a little lower than the test results.
KEYWORDS: reinforced concrete, shear wall, eccentricity, tensile axial force, shear strength

1. INTRODUCTION

When high-rise buildings receive a seismic force, columns at the first story level are subjected to large varying axial forces generated by an overturning moment effect. At the first story of structural walls within such high-rise buildings, it is considered that a boundary column on the compression side for a lateral force may suffer a large tensile axial force generated by the overturning moment effect of the orthogonal direction because seismic forces could be applied from any direction. As well as the walls within these high-rise buildings, walls on the tension side of a non-planar wall like an L-shaped wall and a coupled shear wall with coupling beams may be subjected to a tensile axial force at a boundary column on the compression side for a lateral force. Reports of research on these walls subjected to a tensile axial force have apparently not been published to date. Therefore, the shear behavior of such walls has not been clarified. In this paper, the lateral loading test of six shear wall models which applied a tensile axial force to a boundary column on the compression side for a lateral force is carried out, and then, the shear behavior of these walls is examined.

2. EXPERIMENTAL PROGRAM

2.1 TEST SPECIMENS

A total of six I-shaped walls were tested to failure. As shown in Fig. 1, all specimens had boundary columns with a 15 cm square section, the overall length of the section of the wall was 150 cm, and the clear height of the wall was 140 cm. Though the thickness of the wall panel was designed with a thickness of 5 cm, actual dimensions of the test specimens were shown in Table 1. Reinforcement wire of 4 mm in diameter was used in each wall panel with three kinds of spacings (10 cm, 7.5 cm and 5 cm). Two kinds of main reinforcing bars 13mm in diameter (eight and six D13) were used in the columns. The square spiral hoops made of the wire 4 mm in diameter with three

＊1 Department of Civil Engineering and Architecture, Muroran Institute of Technology, Japan

＊2 Graduate Student, Muroran Institute of Technology, Japan

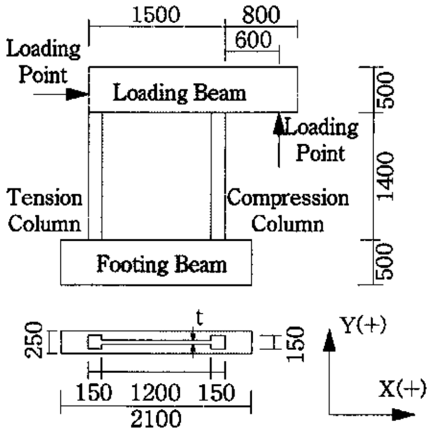

Fig. 1 Details of Specimens (mm)

Table 1 Specimens and Bar Arrangement

Specimens	Thickness of Wall Panel t (mm)	Shear Reinforcement for Wall		Main Reinforcement for Column		Shear Reinforcement for Column		Calculated Strength at Designed Specimen(kN)	
		Bar Arrangement	Ratio Ps(%)*	Bar Arrangement	Ratio Pg(%)	Bar Arrangement	Ratio Pw(%)	Bending Strength	Shear Strength
I-L85	47	4φ@100	0.27	8-D13	4.50	4φ@50	0.34	374	258
I-L83	46	4φ@100	0.28	8-D13	4.50	4φ@30	0.57	374	258
I-L87	49	4φ@100	0.26	8-D13	4.50	4φ@70	0.25	374	258
I-M85	48	4φ@75	0.36	8-D13	4.50	4φ@50	0.34	379	264
I-H85	52	4φ@50	0.50	8-D13	4.50	4φ@50	0.34	388	277
I-L65	53	4φ@100	0.24	6-D13	3.38	4φ@50	0.34	285	244

* Ratio to actual thickness of Wall Panel

Table 2 Properties of Concrete

Specimens	Compressive Strength (N/mm^2)	Tensile Strength (N/mm^2)	Secant Modulus of Elasticity (N/mm^2)
I-L85	20.9	2.13	18500
I-L83	20.7	2.26	19400
I-L87	20.0	2.27	20400
I-M85	20.6	2.06	20600
I-H85	20.5	2.33	19200
I-L65	21.0	2.23	21000

Table 3 Properties of Reinforcement

Size	Cross-sectional Area (cm^2)	Yielding Strength (N/mm^2)	Tensile Strength (N/mm^2)	Elongation Percentage (%)
D22	3.87	387	604	24
D13	1.267	352	497	28
4φ	0.129	221*	293	43

* Yield Stress at Permanent Strain 0.2%

kinds of spacings (7 cm, 5 cm and 3 cm) were used in the columns. Details of the reinforcement for test specimens are shown in Table 1. All the specimens were designed to fail in shear. Calculated values of the bending and shearing strength at the design stage are also shown in Table 1. This bending strength is the value calculated considering both the bending moment caused by the eccentric tensile axial force at the top of the wall and the moment obtained by Eq. (2) shown in Table 5 at the bottom of the wall. This shear strength is the calculated value given by Eq. (3) shown in Table 5 assuming that the axial stress is equal to 0 N/mm^2. All the specimens had two loading beams with a 25 cm × 50 cm section. Longitudinal bars of 22 mm in diameter (six D22) and plain shear reinforcement 13 mm in diameter with a spacing of 8cm were used in these beams. Normal concrete with a maximum aggregate size of 10 mm was used for the test specimens. All the specimens were horizontally cast in forms. The material properties are given in Tables 2 and 3.

2.2 TEST PROCEDURE AND INSTRUMENTATION

As shown in Fig. 2, the lateral and longitudinal forces were applied by two hydraulic actuators named as ① and ②, respectively. In the first place, actuator ① restricted a lateral displacement at the top of the wall, and a longitudinal force was added to a prescribed force by actuator ②. In the next place, actuator ① produced a monotonous gradual increment of a lateral deflection, while applied longitudinal force at the first stage was kept constant by actuator ②. As shown in Fig. 3, the longitudinal force added to each specimen was made to be 80% of values of the longitudinal force P_y. This P_y was the calculated value assuming that the moment M_T made by this P_y at the top of the wall was equal to bending yield moment M_y [2] which was calculated taking this P_y as an axial force. The lateral displacements of the loading beam were measured, and longitudinal displacements of each column and vertical loading point were measured referring to the hooting beam, as shown in Fig. 4. The elongations and the lateral displacements of each column were measured at marked points dividing the wall height into six portions. The strains in the main reinforcing bar of columns and beams were measured by wire strain gauges, and the strains in the spiral hoops at the bottom of the compression column were also measured.

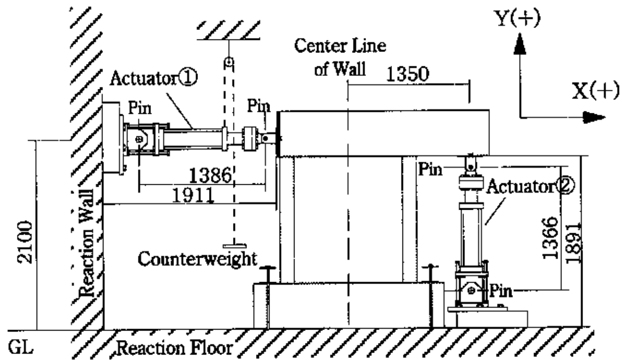

Fig. 2 Loading Apparatus (mm)

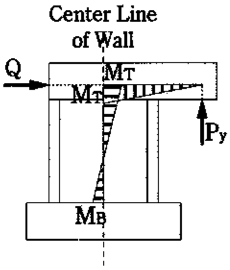

Yielding Moment Equation [1]

$$My = 0.8a_t \cdot \sigma_y \cdot D + 0.2a_w \cdot \sigma_{wy} \cdot D + 0.5N \cdot D\left(1 - \frac{N}{B \cdot D \cdot Fc}\right) \quad \cdots (1)$$

where $N = -Py$

Fig. 3 Moment Distribution

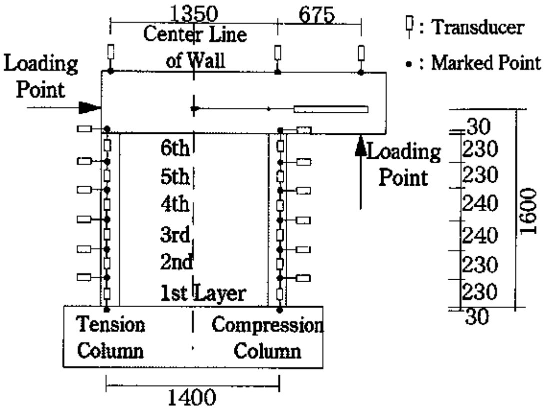

Fig. 4 Measuring Points of Displacement (mm)

3. TEST RESULTS AND DISCUSSION

3.1 FRACTURE PROCESSES

Figure 5 gives the cracking patterns of walls after failure. The diagonal cracks started to appear at the top of the wall near the compression column and at the bottom corner of the wall of the tension column side, while a longitudinal tensile force had been increased. In five specimens except for I-L83, diagonal cracks inclined about 45° occurred near the diagonal line and at the under side of the diagonal line of the wall, when the lateral deformation at the top of the wall began to gradually increase. Then the width of the inclined cracks near the diagonal line gradually was widened with an increase in the lateral deformation. At the maximum lateral load, the walls failed in shear when many inclined cracks occurred suddenly at both the bottom of the compression column and the top of the

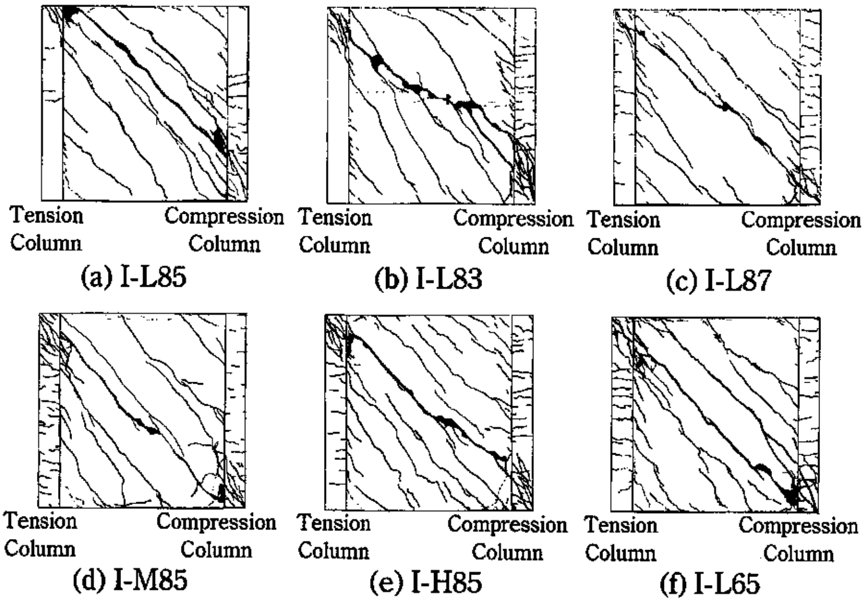

Fig. 5 Cracking Patterns

tension column, and the opening of the inclined cracks of the wall was observed. I-L83 had the lateral crack shown by a dotted line in Fig. 5 at the center of the wall height before the test started. In the case of I-L83, this lateral crack was connected with inclined cracks that occurred at boundary columns, and a opening of the crack which had a gentle inclination compared to cracks of other specimens was observed as the lateral displacement increased. This wall failed in shear at the maximum load when an opening of the shear cracks at both the bottom of the compression column and the top of the tension column were observed. The range of the inclined cracks that occurred at the bottom of the compression column had enlarged upward in comparison with other test specimens. Observing the yield situation of the reinforcements, though a part of the main reinforcement at both the bottom of the compression column and the top of the tension column yielded on all the specimens, the greater part of main reinforcements of columns did not yield.

3.2 LOAD-DEFLECTION CURVES

Figure 6 shows the relationships between the lateral load, Qx, and the drift angle, Rx, at the top of the walls. After the maximum lateral loads were reached, the load carrying capacity reduced rapidly due to the shear failure of the walls accompanied with openings of the already formed shear cracks of the columns. However, the lateral load of I-L83 was lower than that of the other specimens, and the proportion of the reduction in the lateral load decreased after the maximum lateral load was reached. It is considered that these are caused by the effect of the lateral crack shown by a dotted line in Fig. 5 and a high shear reinforcement ratio of boundary columns. Comparisons of the lateral load-deflection curves are shown in Fig. 7. According to Fig. 7(a), before the maximum lateral loads were reached, though the curves of two specimens except for I-L83 almost agreed, the maximum load of I-L85 with higher shear reinforcement was slightly larger than that of I-L87 with lower shear reinforcement. And the deformation at the maximum load of I-L85 was also larger than that of I-L87. According to Fig. 7(b), though the maximum loads of both I-M85 and I-H85 with high shear reinforcement ratios within wall panels were a little larger than that of I-L85 with the lowest shear reinforcement within a wall panel, there was no clear difference among three curves as a shear reinforcement ratio within a wall panel changed. According to Fig. 7(c), before the maximum lateral loads were reached, the difference between two curves was not almost observed but the maximum load of I-L85 with higher main reinforcement ratio of columns was slightly larger than that of I-L65.

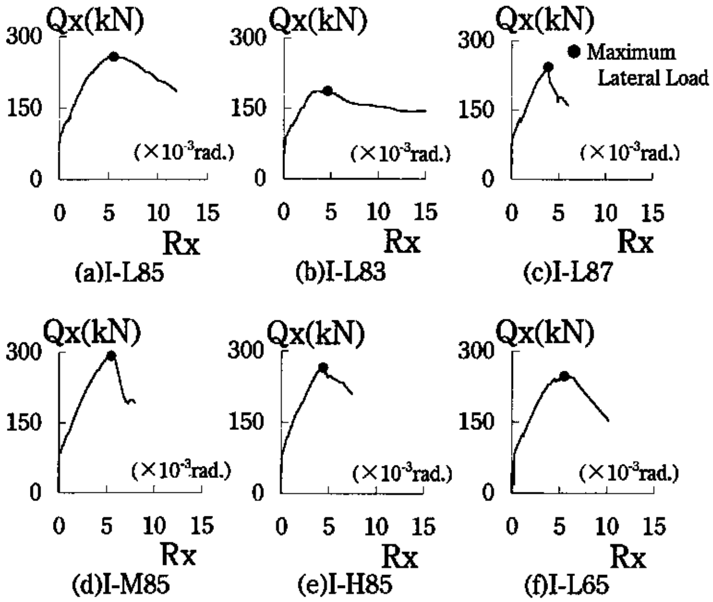

Fig. 6 Load-Deflection Curves

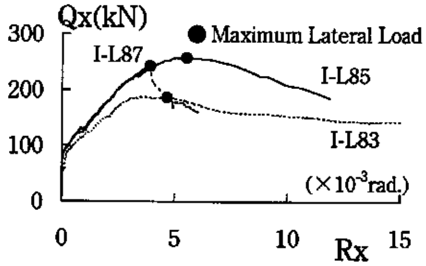

(a) Influence of Shear Reinforcement Ratio of Column

(b) Influence of Shear Reinforcement Ratio within Wall Panel

(c) Influence of Main Reinforcement Ratio of Column

Fig. 7 Comparisons of Load-Deflection Curves

3.3 ELONGATIONS AND LATERAL DISPLACEMENTS

Figure 8 shows the deformations measured by variable transducers mounted at boundary columns as shown in Fig. 4. In Fig. 8, the deformations at finishing the increment of the longitudinal force and around the maximum lateral load are shown. According to Fig. 8, while the longitudinal force was added to the prescribed force, the compression column was extended. However, the elongation and lateral displacement were hardly observed at the tension column. When the lateral displacement at the top of the wall began to increase, the tension column was extended as the lateral deformation at the top of the wall increased. And the elongation at both the top and bottom of this column was large. The lateral displacement of the tension column gradually increased with the change to the upper layer from the lower layer, and the relative layer displacements of this column became greater than the lower layer. Especially, the relative layer displacement of the most upper layer rapidly increased in comparison with that of the other layers after the maximum lateral loads were reached. On the other hand, the elongations of the compression column were kept constant, and the elongations of the tension column at the maximum lateral load were almost the same values as those of the compression column. Though the lateral displacement of the compression column was as large as the upper layer, the differences of the displacements appeared to 4th layer from 6th layer were small and the relative layer displacement was larger as a lower layer. After the maximum lateral load was reached, the lateral displacements of the 1st and 2nd layer increased. Especially, the relative layer displacement of the 1st layer rapidly increased on five specimens except I-L83. The relative layer displacement of I-L83 rapidly grew at not only 1st layer but also 2nd layer, an opening of the inclined cracks at the bottom of the compression column corresponded to this.

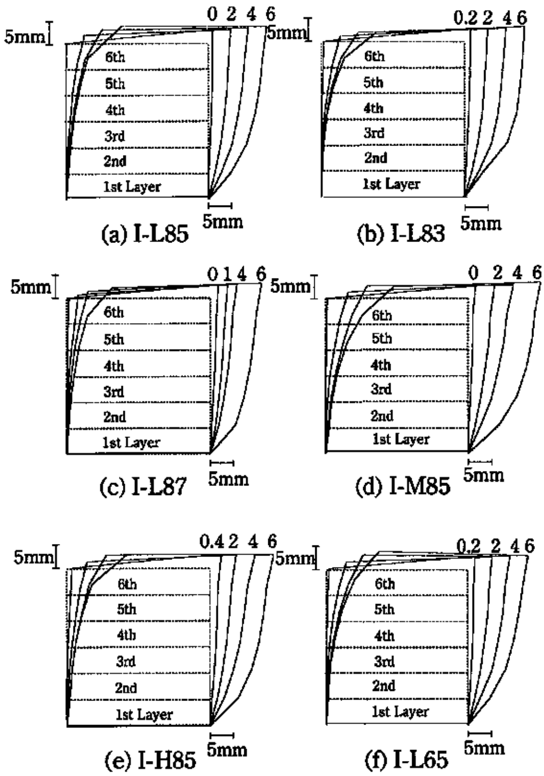

Figures; Drift Angle ($\times 10^{-3}$rad.)

Fig. 8 Deformation Diagrams

3.4 SHEAR STRENGTH

Table 4 lists the maximum test values, $_tQ_{max}$, and four kinds of calculated values. In addition, the eccentric tensile force, P, and the drift angle, R, at the maximum lateral load are also shown in the Table 4. The calculated value $_cQ_{bu}$ is the bending strength calculated considering both the moment caused by the eccentric tensile force P at the top of the wall and the moment obtained by Eq. (2) [2] shown in Table 5 at the bottom of the wall. The calculated value $_cQ_{su1}$ is given by Eq. (3) [2] shown in Table 5 assuming that the axial stress σ_0 is equal to 0 N/mm^2. Shear span M/Q is calculated from the bending moment distributions given by both the eccentric tensile force P and the test value of $_tQ_{max}$. These moment distributions are shown in Fig. 9. The calculated value V_u is obtained from Eq. (4) [3] shown in Table 5. According to Table 4, though each calculated value becomes greater as the value of shear reinforcement ratio p_s within a wall panel increases, the test value of I-H85 (p_s=0.50%) is smaller than that of I-M85 (p_s=0.36%). In I-H85, it is considered that the strength is developed when the compression column fails in shear before all shear reinforcements within a wall panel yield. Here, a test value is compared with a calculated value

Table 4 Ultimate Strength

Specimens	Test Value				Calculated Value				Ratio			
	tQmax (kN)	P (kN)	σ0 (N/mm^2)	R (10^{-3}rad.)	cQbu (kN)	cQsu1 (kN)	cQsu2 (kN)	Vu (kN)	tQmax / cQbu	tQmax / cQsu1	tQmax / cQsu2	tQmax / Vu
I-L85	258	-166	-1.63	5.50	374	255	241	205	0.69	1.01	1.07	1.26
I-L83	187	-166	-1.65	4.63	374	252	238	199	0.50	0.74	0.79	0.94
I-L87	243	-165	-1.59	3.88	374	254	240	205	0.65	0.96	1.01	1.19
I-M85	292	-165	-1.61	5.50	378	261	248	213	0.77	1.12	1.18	1.37
I-H85	265	-169	-1.57	4.38	388	283	269	245	0.68	0.94	0.99	1.08
I-L65	247	-129	-1.19	5.50	287	254	243	227	0.86	0.97	1.02	1.09
Average	—	—	—	—	—	—	—	—	0.69	0.96	1.01	1.16

including I-H85. Ratio of the test result $_tQ_{max}$ to calculated value $_cQ_{su1}$ ranges from 0.74 to 1.12 with an average of 0.96 (its deviation is 11.8%). $_cQ_{su1}$ slightly exceeds $_tQ_{max}$. Then, $_cQ_{su2}$ is calculated by Eq. (3) [2] shown in Table 5 as well as $_cQ_{su1}$ using the actual axial negative stress σ_0 which occurs by the eccentric tensile force P. The ratio of $_tQ_{max}$ to $_cQ_{su2}$ ranges from 0.79 to 1.18 with an average of 1.01 (its deviation is 11.5%). Therefore, $_cQ_{su2}$ considering a tensile force is more similar to the test result than $_cQ_{su1}$ disregarding a tensile force. The ratio of $_tQ_{max}$ to V_u ranges from 0.94 to 1.38 with an average of 1.16 (its deviation is 12.0%). V_u underestimates the test value by about 16%.

Table 5 Strength Equations

Bending Strength [2]

$$M_{bu} = 0.9a_t \cdot \sigma_y \cdot D + 0.4a_w \cdot \sigma_{wy} \cdot D + 0.5N \cdot D\left(1 - \frac{N}{B_c \cdot D \cdot F_c}\right) \quad \cdots(2)$$

Shear Strength [2]

$$Q_{su1} = \left\{\frac{0.068 p_{te}^{0.23}(F_c + 180)}{\sqrt{M/(Q \cdot D) + 0.12}} + 2.7\sqrt{\sigma_{wh} \cdot p_{wh}} + 0.1\sigma_0\right\} b_e \cdot j \quad \cdots(3)$$

Shear Strength ("AIJ Design Equation" [3])

$$V_u = t_w \cdot l_{wb} \cdot p_s \cdot \sigma_{sy} \cdot \cot\phi + \tan\theta(1-\beta) t_w \cdot l_{wa} \cdot \nu \cdot \sigma_B / 2 \quad \cdots(4)$$

here $\tan\theta = \sqrt{(h_w/l_{wa})^2 + 1} - h_w/l_{wa}$

$\nu = 0.7 - \sigma_B/200$

h_w : height of loading point from hooting beam

Please refer to references for each symbol.

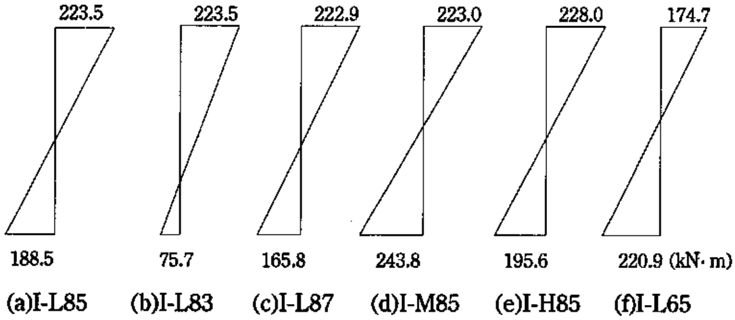

Fig. 9 Bending Moments at Maximum Lateral Load

4. CONCLUSIONS

Based on the test results of shear walls under an eccentric tensile axial force, the following conclusions can be made.

(1) The calculated value by shear strength Eq. (3) [2] using actual axial negative stress agreed almost with the test result. Therefore, it was apparent that this equation could be used as the shear strength equation of the wall subjected to an eccentric tensile axial force.

(2) The calculated value obtained from Eq. (4) [3] underestimated the test value by about 16%.

However, because this test adopts monotonous loading and the test specimens are few, it is necessary to continue investigation on these.

ACKNOWLEDGMENT

This investigation was supported by the 1999 Grant-in-Aid for Scientific Research, Ministry of Education, Science and Culture of Japan.

REFERENCES

(1) Hirosawa, M., "Past Experimental Results on Reinforced Concrete Shear Walls and Analysis on them," Kenchiku Kenkyu Shiryo, No.6, Mar. 1975, pp.33-34.

(2) AIJ, "Ultimate Strength and Deformation Capacity of Buildings in Seismic Design (1990)," 1990, pp.401-403.

(3) AIJ, "Design Guidelines for Earthquake Resistant Reinforced Concrete Buildings Based on Inelastic Displacement Concept," 1999, pp.209-214.